

# Fabrication of bulk Al-La-Ni alloy by spark plasma sintering

C. Y. XÜ, S. S. JIA\*, Z. Y. CAO

Key Laboratory of Automobile Materials of Education and Department of Materials Science and Engineering, Jilin University, Changchun 130025, People's Republic of China  
E-mail: [jjass@jlu.edu.cn](mailto:jjass@jlu.edu.cn)

Published online: 12 January 2006

The bulk Al<sub>85</sub>La<sub>10</sub>Ni<sub>5</sub> alloy is sintered by spark plasma sintering (SPS) method. The microstructure and mechanical properties of the Al<sub>85</sub>La<sub>10</sub>Ni<sub>5</sub> samples are investigated. The results show that the bulk Al<sub>85</sub>La<sub>10</sub>Ni<sub>5</sub> alloy with less than 1.5% porosity has been obtained at 693 K. The hardness of the alloy sintered at 693 K reaches HRB 98 and the wear resistance of the alloy is twice of the conventional A390 aluminum alloy. The high wear resistance of aluminum alloy is attributed to second-phase strengthening.

© 2006 Springer Science + Business Media, Inc.

## 1. Introduction

Considerable effort has been devoted to the development of novel lightweight engineering materials during the last decades [1, 2]. Such Al alloys in recent years have received considerable attention especially in automobile and aerospace industries due to their low density and high specific strength and good wear resistance. In the recent research, various amorphous alloys with high Al content (Al ≥ 85at%) have shown good mechanical property [3, 4]; in particular, Al-Ln-Tm (Ln = rare earth, Tm = V, Cr, Mn, Fe, Mo) amorphous aluminum alloys of melt-spun ribbons possess high strength and good toughness [5–7]. The tensile strengths of such alloys are more than 1000 MPa while the highest strength reaches 1250 MPa. If the α-Al nanoparticles or icosahedral quasicrystals were used as a strengthening phase in an amorphous matrix, the strength of the alloy further improves [8–11].

The shapes of the amorphous alloys are, however, limited to ribbon, wire, film and powder, since the synthesis of these alloys requires high cooling rates from the melts [12]. Their small size makes engineering application unlikely. For this reason, hot pressing and/or hot extrusion methods were recently used to fabricate bulk samples [9–14]. However, a large pressure (> 1 GPa) and a sufficiently high pressing temperature are needed. Spark plasma sintering (SPS) is a recent innovation in activated sintering and densification by charging a high-pulsed electric current directly through the powders in a die under externally applied pressure [15, 16]. SPS allows very fast heating and cooling rates, very short holding time, and the possibility

to obtain fully dense samples at comparatively low sintering temperatures, typically a few hundred degrees lower than normal hot pressing [17].

In the present contribution, bulk Al<sub>85</sub>La<sub>10</sub>Ni<sub>5</sub> alloy samples were sintered at a suitable temperature and pressed using SPS method; the microstructure, porosity, hardness and wear resistance of the alloy were investigated.

## 2. Experimental methods

The alloy was prepared from Al, La, and Ni with a purity of 99.9%. The constituents with a designed composition of Al<sub>85</sub>La<sub>10</sub>Ni<sub>5</sub> (at%) were melted together in a vacuum induction furnace under an argon atmosphere. Alloy powders with a particle size ranging from 5 to 40 μm were obtained by ultrasonic atomization with a cooling rate of about 10<sup>3</sup> Ks<sup>-1</sup>. The powders were poured into a WC-Co die with 20 mm inner diameter. First, the powder in the die was pressed under a uniaxial pressure of 45 MPa at ambient temperature, and then the die was put into the chamber of the SPS machine. The sample was heated with a heating rate of 100 K/min to the temperature of 573, 623, 693, 773 and 793 K in a vacuum of 5–10 Pa for a hold time of 5 min, respectively. During the SPS processing, a uniaxial pressure of 100 MPa was applied upon the sample through the graphite punches. A cooling rate of 40 K/min was used. The working temperature was measured using a thermocouple pyrometer.

The microstructures were investigated by using scanning electron microscopy (SEM). The phase structure

\* Author to whom all correspondence should be addressed.

analysis of the sintering samples was made by X-ray diffraction (XRD). The hardness of the samples was measured by a Rockwell hardness instrument. Wear tests were conducted in air on a pin-on-disc machine. The test pin was loaded against the disc with a dead weight. The size of pin was 6 mm in diameter and 12 mm in length. The counter face disc, 70 mm in outside diameter and 10 mm in thickness, was fabricated using E52100 bearing steel (composition in mass%: 1.0C, 0.35Mn, 0.3Si, 1.4Cr, balance Fe) with a bulk hardness of HRC  $62 \pm 2$ . The pin and the disc were washed with acetone to ensure that the tests were carried out under a nominally dry sliding condition. A photoelectric balance with a precision of 0.01 mg was used to measure the weight of the pin before and after each test. Tests were carried out at a constant sliding velocity of 0.942 m/s and the loading range was between 20 N and 120 N, with a sliding distance of 942 m. Each test was repeated five times and the results were averaged. The density of the sintered samples was measured using Archimedes principle with a photoelectric balance with a precision of 0.01 mg. The porosity of the alloy ( $\delta$ ) was then determined as follows:

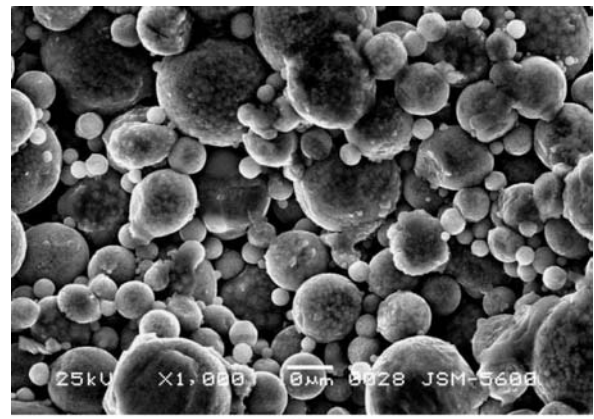
$$\delta = (\rho_t - \rho_m) / \rho_t \quad (1)$$

where  $\rho_m$  and  $\rho_t$  are the measured density of the alloy and the theoretical density from the density of the constituent elements respectively.

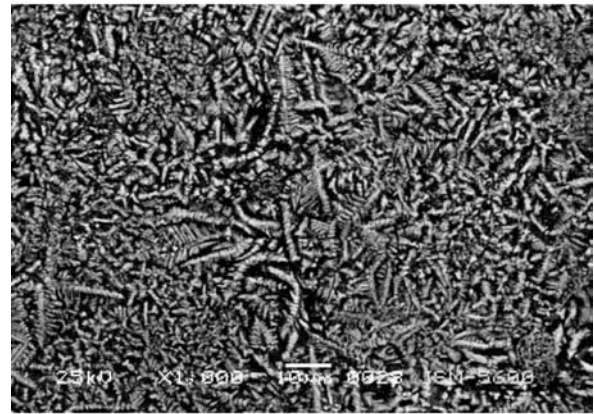
### 3. Results and discussion

Fig. 1 shows the SEM microstructures of bulk alloys with different sintering temperature. When the sintered temperature was 573 K, the microstructure retained the original spherical powder form in diameter of 5–30  $\mu\text{m}$ , which indicates that a bulk sample could not be formed at 573 K, at which the sintered powders have been not bonded during the SPS. Only when the sintering temperature reaches 693 K, could it be seen that the original shape of powder particles had disappeared, crystallization has occurred and microscopic porosity is hardly evident, so a full re-crystallized structure was obtained with typically dendritic features. The microstructure sintered at 773 K is coarser than that of at 693 K, which indicates that the growth of grain and coarsening of intermetallic compounds occur. The corresponding porosity of the alloys changes as a function of the sintering temperature  $T$  is presented in Fig. 2 that supports the above observation. As sintering temperature increases from 573 to 693 K, the porosity of the bulk alloy significantly decreases. However, at sintering temperatures ranging from 693 to 793 K, the porosity remains nearly constant at less than 1.5%.

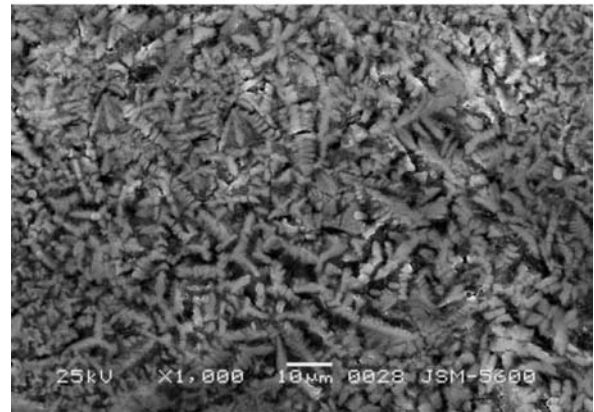
X-ray analysis of the sample at 693 K shows the presence of  $\alpha$ -Al,  $\text{La}_3\text{Al}_{11}$ ,  $\text{Al}_4\text{La}$ ,  $\text{LaNi}_3$ ,  $\text{Al}_3\text{Ni}$  and  $\text{Al}_2\text{O}_3$ , as shown in Fig. 3. The appearance of the above intermetallic compounds and oxides should contribute to the hardness of the alloys.



(a)



(b)



(c)

Figure 1 SEM micrographs of sample sintered at temperatures of (a) 573 K, (b) 693 K and (c) 773 K.

Fig. 4 shows the hardness of the alloy as a function of sintering temperature ( $T_s$ ). The Rockwell hardness value is the highest at 693 K, HRB = 98. However, it is interesting to note that further increase of  $T_s$  leads to drop of the Rockwell hardness. The decrease of the hardness may be induced by grain growth or coarsening of intermetallic compounds at high temperature that can be seen in Fig. 1b and c. It should be noted that the decrease of the hardness may be induced by the grain growth or the coarsening intermetallic compounds at high temperature. In addition, note that the lowest sintering

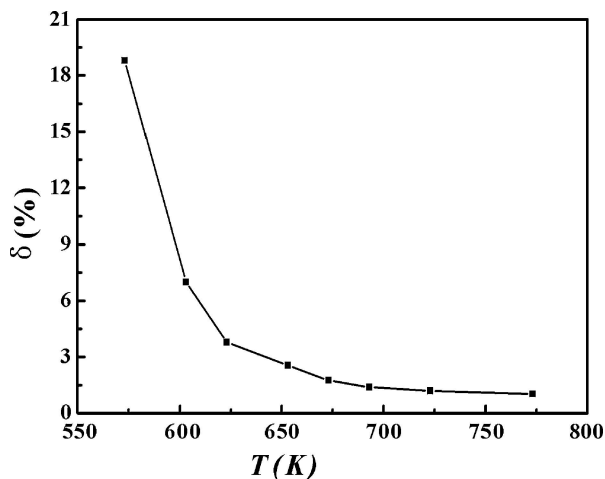


Figure 2 Porosity of the alloys as a function of sintered temperature.

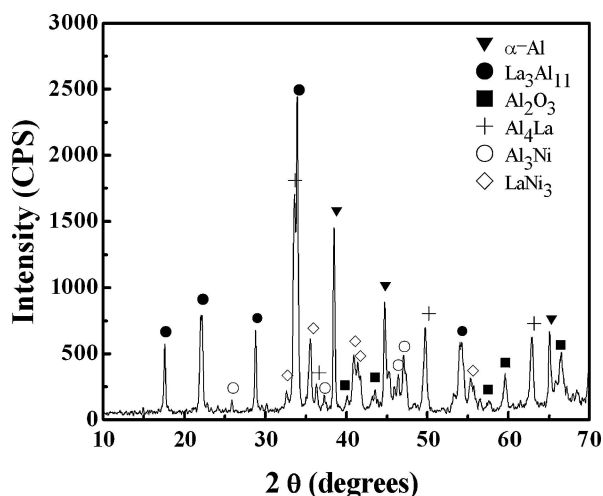


Figure 3 X-ray structure analysis of the alloy sintered at 693 K.

temperature where Rockwell hardness can be measured is 623 K (when  $T_s < 623$  K, the sample is too brittle to resist the deformation induced by the indenter of the hardness experiment). Grain growth could arise from two aspects. First, the applied pressure would accelerate any dynamic grain growth; second, the spark discharge happened between the particles and would largely increase the surface activity of the particles, which would then accelerate surface diffusion and make the grains grow [18].

Only after a fresh surface of the alloy could be contacted directly, could the compacted alloy be obtained by compression. However, the surface of the powders is covered with alumina film during both manufacture and storage. Since the alumina has a higher melting temperature, if the bulk alloy is prepared by a normal powder metallurgy method, a higher pressure ( $>1$  GPa) and higher sintering temperatures are needed to break the alumina films on the surface of the powders. By using SPS, a strong electrical field is produced in the small gaps between the particles and the momentary high-temperature field generated by pulse energy, spark impact pressure and electrical resistance heating [19, 20]. A lo-

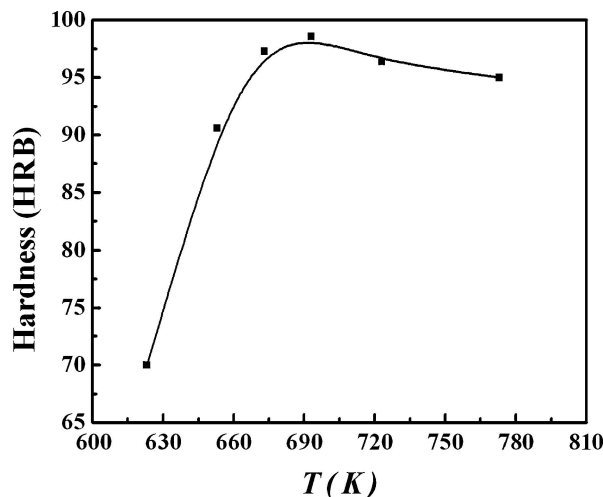


Figure 4 Rockwell hardness measurement results for the bulk alloy as a function of sintering temperature.

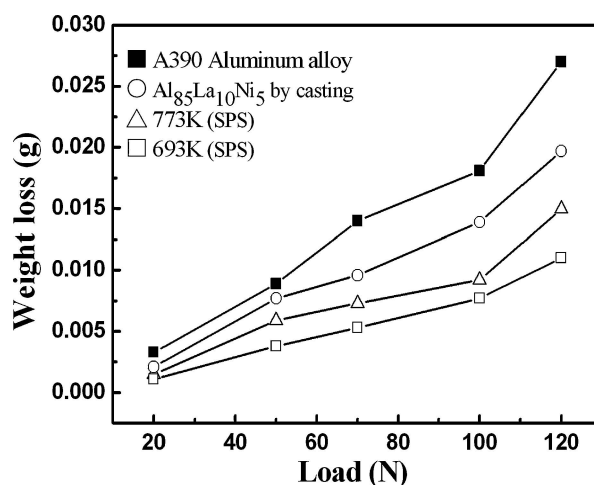


Figure 5 Wear curves of the alloys sintered at different temperatures with increasing load.

cally high temperature is created in the contacting areas of the particles where aluminum oxide films are ruptured by the spark plasma [15], so that the fresh surfaces of the powder particles are in contact directly. At the same time, the spark discharges may bring about evaporation and melting of the surface of the powder particles, thus inducing neck formation, growth and contact flattening [21]. As a result, a compacted bulk alloy can be obtained.

Since the high hardness of the alloy may be accompanied by high wear resistance, the wear curve of the alloys is shown in Fig. 5. The hardness values of the alloy sintered by SPS are 98 HRB at 693 K, while the hardness of the casting  $Al_{85}La_{10}Ni_5$  and A390 alloys are 82 HRB and 71 HRB respectively. The wear resistance of the  $Al_{85}La_{10}Ni_5$  alloys by SPS is higher than those of casting  $Al_{85}La_{10}Ni_5$  alloy and A390 alloy due to the high hardness of the alloy by SPS. The alloy sintered by SPS at 693 K exhibits the best wear resistance among the alloys, which is twice that of the A390 aluminum alloy. The

good wear resistance of the alloy is attributed to the large amount of intermetallic compound present in the samples.

#### 4. Summary

A high density of bulk Al<sub>85</sub>La<sub>10</sub>Ni<sub>5</sub> alloy with porosity less than 1.5% can be prepared by spark plasma sintering at 693–793 K, sintering time of 5 min and pressure of 100 MPa. The highest hardness of the sintered alloy reaches HRB 98 at 693 K, while a further increase of sintering temperature leads to drop of hardness of the alloy due to coarsening of the intermetallic compounds. The wear resistance of the alloy sintered at 693 K is twice as high as that of the conventional A390 alloy.

#### Acknowledgments

The financial support from Chinese National Key Basic Research and Development Program (Grant No. 20004CB619301) is acknowledged.

#### References

1. F. SCHURACK, J. ECKERT and L. SCHULTZ, *Acta Mater.* **49** (2001) 1351.
2. Q. C. JIANG, H. Y. WANG, Q. F. GUAN and X. L. LI, *Adv. Eng. Mater.* **5** (2003) 722.
3. M. WATANABE and A. INOUE, *Mater. Trans., JIM.* **34** (1993) 162.
4. A. TOKAR, L. LEVIN and Z. METALLKD, **89** (1998) 16.
5. A. INOUE, *Acta Mater.* **48** (2000) 279.
6. M. TAKAGI, H. OHTA, T. IMURA and A. INOUE, *Scr. Mater.* **44** (2001) 2145.
7. A. INOUE, *Prog. Mater. Sci.* **43** (1998) 365.
8. R. MANAILA, D. MACOVEI, R. POPESCU, A. DEVENYI, A. JIANU, E. VASILE, P. B. BARNA and J. L. LABAR, *Mater. Sci. Eng.* **A294/296** (2000) 82.
9. A. INOUE and H. KIMURA, *J. Light Metals.* **1** (2001) 31.
10. J. C. LI, Z. K. ZHAO and Q. JIANG, *Mater. Sci. Eng.* **A339** (2003) 205.
11. *Idem.*, *Adv. Eng. Mater.* **5** (2003) 119.
12. Y. KAWAMURA, H. MANO and A. INOUE, *Scr. Mater.* **44** (2001) 1599.
13. F. SCHURACK, J. ECKERT and L. SCHULTZ, *Mater. Sci. Eng.* **A294/296** (2000) 164.
14. Z. K. ZHAO, J. C. LI and Q. JIANG, *J. Mater. Eng. Perform.* **11** (2002) 262.
15. M. OMORI, *Mater. Sci. Eng.* **A287** (2000) 183.
16. G. D. ZHAN, J. KUNTZ, J. WAN, J. GARAY and A. K. MUKHERJEE, *Scr. Mater.* **47** (2002) 737.
17. M. NYGREN and Z. J. SHEN, *Solid State Sci.* **5** (2003) 125.
18. W. LI and L. GAO, *J. Eur. Ceramic. Soc.* **20** (2000) 2441.
19. Y. C. WANG and Z. Y. FU, *Mater. Sci. Eng.* **B90** (2002) 34.
20. K. A. KHOR, K. H. CHENG, L. G. YU and F. BOEY, *ibid.* **A347** (2003) 300.
21. J. LIU, A. LAL and R. M. GERMAN, *Acta Mater.* **47** (1999) 4615.

*Received 3 January  
and accepted 31 May 2005*